Available online at www.sciencedirect.com
SCIENCE DIRECT®
Journal of Photochemistry and Photobiology A: Chemistry 164 (2004) 75–80
Journal of Photochemistry and Photobiology A:Chemistry
www.elsevier.com/locate/jphotochem

Photosensitization of nanostructured TiO_2 with CdSe quantum dots: effects of microstructure and electron transport in TiO_2 substrates

Qing Shen, Dai Arae, Taro Toyoda*

Department of Applied Physics and Chemistry, The University of Electro-Communications, 1-5-1 Chofugaoka, Chofu, Tokyo 182-8585, Japan

Received 25 July 2003; received in revised form 7 December 2003; accepted 14 December 2003

Abstract

Four sample types of nanostructured titanium dioxide (TiO_2) electrodes were studied, variously prepared with TiO_2 nanocrystalline particles of different sizes (15 and 27 nm in diameter) and with the addition of polyethylene glycol (PEG) binders having two different molecular weights (MW) (20,000 and 500,000). CdSe nanoparticles (CdSe quantum dots: CdSe QDs) were adsorbed on to each of the four types of TiO_2 electrode using a chemical deposition technique. Photoacoustic (PA) and photoelectrochemical (PEC) current spectra were measured, together with the incident photon to current conversion efficiency (IPCE). The photosensitization by the CdSe QDs was confirmed. It was found that the PEC current and IPCE are strongly dependent on the TiO_2 nanoparticle size and the MW of PEG in the TiO_2/water paste. The correlation of the PEC and IPCE with the microstructure and the electron diffusion coefficient for each of TiO_2 nanostructured electrode type are discussed, providing information which could lead to the optimization of dye-sensitized solar cells (DSSC).

Keywords: Nanostructured; TiO_2; CdSe quantum dot; Photoacoustic (PA); Photoelectrochemical (PEC) current; Electron transport

1. Introduction

Nanocrystalline titanium dioxide (TiO_2) has received considerable attention in numerous fields of application such as in photoelectrochemical (PEC) solar cells, photocatalysis and in gas sensors. In particular, significant progress has been made by Grätzel and co-workers since the 1990s [1,2] in solar cell fabrication using nanostructured TiO_2 electrodes coated with organic dyes, resulting in the so-called dye-sensitized solar cell (DSSC) or Grätzel cell. The Grätzel cell exhibits a high solar energy conversion efficiency, exceeding 10%, and good long-term stability. Along with the research on the electrolyte and adsorption dyes, interest in the preparation and characterization of nanostructured TiO_2 electrodes has grown rapidly in recent years, following the discovery that the efficiency of the DSSC was significantly dependent on the properties of the nanostructured TiO_2 [3]. These electrodes can be made from a solution or a paste containing TiO_2 nanoparticles of the desired size [4,5]. In addition to organic dyes, narrow-band-gap semiconductor nanocrystals, such as CdS and PbS, have attracted significant interest as light harvesters in DSSCs [6–10]. The use of semiconductor nanocrystals as sensitizer has some advantages in solar cell applications. Firstly, the band gap of the nanocrystals can be tuned by controlling their size so that the absorption spectrum can be tuned to match the spectral distribution of sunlight and a full-spectrum solar cell can be fabricated more easily. Secondly, nanocrystals have a large extinction coefficient due to quantum confinement and intrinsic dipole moments, leading to rapid charge separation. Thirdly, semiconductor nanocrystals have a robust inorganic nature [11].

To optimize the DSSC for high efficiency, it is important to study the optical absorption, charge injection, carrier transport and recombination of TiO_2 electrodes, as well as the correlation between these attributes and morphologies. Hence, control of morphology and interfacial properties is essential for DSSC fabrication. In a previous paper [12], we reported the experimental results of photoacoustic (PA) [13–15] and photoelectrochemical (PEC) current [16–18] measurements obtained from four samples of nanocrystalline TiO_2 electrode prepared from TiO_2/water pastes, containing different nanometer-size TiO_2 powders (15 and 27 nm in diameter) and with the addition of polyethylene glycol (PEG) binders having different molecular weights (MW) (20,000 and 500,000). The PA method is a photothermal detection technique, which has been proven to be powerful for the investigation of the optical absorption and thermal properties of various materials by measurement of

* Corresponding author. Tel.: +81-424-43-5464; fax: +81-424-43-5501.
E-mail address: toyoda@pc.uec.ac.jp (T. Toyoda).

1010-6030/$ – see front matter © 2004 Elsevier B.V. All rights reserved.
doi:10.1016/j.jphotochem.2003.12.027

nonradiative de-excitation processes. It is useful for measurements in optically opaque or scattering solid materials, which are difficult or impossible to investigate using conventional optical absorption measurements. In the previous work [12], we also presented qualitative experimental results of the electron transport in the nanostructured TiO_2 electrodes, using photocurrent transient (PCT) [19,20] measurements. In order to investigate the optimum combination of TiO_2 nanoparticle size and PEG molecular weight, we adsorbed CdSe nanoparticles (CdSe quantum dots: CdSe QDs) onto the nanostructured TiO_2 electrode samples and measured PA, PEC current spectra and incident photon to current conversion efficiency (IPCE). We also investigated the electron transport in the TiO_2 electrodes in some detail in order to interpret the experimental results. In this paper, we report on the effects of microstructure and electron transport in TiO_2 substrates on the photosensitization of nanostructured TiO_2 by CdSe QDs.

2. Experimental

The method of preparation of TiO_2 electrodes has been reported in a previous paper [12]. Four samples of TiO_2 paste were prepared with different sized TiO_2 nanocrystalline particles (Super Titania: Showa Denko; anatase structure) (15 and 27 nm in diameter) and different polyethylene glycol molecular weights (20,000 and 500,000) (defined as A-(a) (15 nm with PEG20000), A-(b) (15 nm with PEG500000), B-(a) (27 nm with PEG20000) and B-(b) (27 nm with PEG500000). The resulting pastes were applied onto indium tin oxide (ITO) coated glass substrates with a Scotch tape as a frame and spacer, raking off the excess solution with a glass rod. The TiO_2 film thickness could be increased by several repetitions of this process. The TiO_2 electrodes were dried in air at room temperature for 10 min, followed by treatment at a temperature of 100 °C for 10 min. This was followed by ramping to 450 °C for 40 min, with a dwell at 450 °C for 30 min before cooling to room temperature. Four sample types with almost the same thickness (8–10 μm) were used for CdSe deposition. The CdSe QDs were prepared using a chemical solution deposition technique, following the procedure published by Gorer and Hodes [21]. Firstly, as the Se source, an 80 mM sodium selenosulphate (Na_2SeSO_3) solution was prepared by dissolving elemental Se powder in a 200 mM Na_2SO_3 solution. Secondly, 80 mM $CdSO_4$ and 120 mM trisodium salt of nitrilotriacetic acid ($N(CH_2COONa)_3$) were mixed in a volume ratio 1:1. Finally, both solutions were mixed in a volume ratio 1:2. TiO_2 electrodes were placed in darkness in a glass container filled with the final solution for a various deposition times (1–120 h). All four types of electrode were deposited using the same solutions. We observed different sizes for dot structure of CdSe by SEM measurements.

The optical absorption of the TiO_2 electrodes with and without CdSe QD deposition was studied using the PA technique. A gas-microphone PA method was used [13]. A 300 W xenon arc lamp was used as a light source. A monochromatic light beam was obtained by passing the light through a monochromator. This beam was modulated with a mechanical chopper and focused on to the surface of a sample placed inside a sealed PA cell. Measurements of the PA spectra were carried out in the wavelength range of 250–800 nm with a modulation frequency of 33 Hz at room temperature. The PA signal was monitored by first passing the microphone output through a preamplifier and then into a lock-in amplifier. PA spectra were normalized using PA signals from a carbon black sheet [14].

The PEC current setup consisted of a quartz cell equipped with a working-electrode (TiO_2) and a Pt counter electrode in 1 M KCl + 0.1 M Na_2S electrolyte [6]. PEC current measurements were carried out under short circuit current conditions using the same apparatus and conditions as those used for the PA measurements. The spectra were normalized using PA signals from a carbon black sheet. The nanostructured TiO_2 electrode was illuminated both from the electrolyte/TiO_2 (front-side illumination) and electrolyte/ITO (back-side illumination) interface sides. The measurement of incident photon to current conversion efficiency was also carried out using the same setup by measuring the short circuit current.

The electron transport in the nanostructured TiO_2 electrodes without CdSe deposition was studied using PCT measurements. The setup consisted of a Nd:YAP (yttrium aluminum perovskite) pulsed laser with a pulse duration of 10 ns and an electrochemical system similar to that used in the PEC measurement. The light of third harmonic generation (THG) from the YAP laser with a wavelength of 359 nm was incident on the TiO_2 electrode and the short circuit current transient was monitored by a digital oscilloscope. The intensity of the THG was 0.5 mJ/pulse. The nanostructured TiO_2 electrode was illuminated from the front-side. The electrolyte was 1 M KCl + 0.1 M Na_2S, as used in PEC measurements.

3. Results and discussion

3.1. PA, PEC and IPCE spectra for CdSe adsorbed TiO_2 electrodes

The formation of CdSe QDs on the TiO_2 electrodes has been confirmed by X-ray diffraction (XRD). Diffraction peaks at $2\theta = 25.5$, 42.4, and 50.0° were observed, corresponding to the (1 1 1), (2 2 0), and (3 1 1) reflections of cubic cadmium selenide. The peaks were very broad in fact, implying that the sizes of CdSe QDs were very small. We estimated the average size of CdSe QDs to be ca. 6 nm from the full width at half maximum of diffraction peaks according to the Scherrer equation [22,23]. In this study, we only present the experimental results of the samples with deposition time of 19 h. Fig. 1 shows PA intensity spectra of CdSe

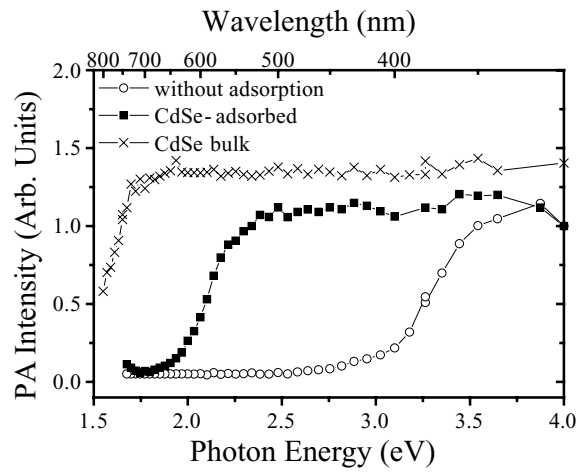

Fig. 1. Photoacoustic spectra of the TiO_2 electrodes (A-(b), (15 nm with PEG500000)) with and without CdSe quantum dots deposition for 19 h and that of bulk CdSe powders.

deposited TiO_2 electrode and that without deposition (the TiO_2 substrates: A-(b)), where the PA intensity amplitudes were normalized at a wavelength of 310 nm (photon energy, 4.0 eV). The red shift of the spectra by CdSe QDs can be clearly observed for the deposited sample. The PA spectrum from commercial bulk CdSe powders with sizes of a few micrometers is also shown in Fig. 1, in which a absorption shoulder appeared at 1.73 eV. This is in good agreement with the band-gap energy E_g of bulk CdSe reported elsewhere [21]. Relative to E_g of the bulk CdSe, the optical absorption shoulder in the PA spectra of CdSe deposited sample shows blue shift. It means that the quantum confinement effect occurred in the CdSe deposited sample, implying that the radius of the CdSe QDs are smaller than the Bohr radius of the exciton in bulk CdSe, i.e., 5.6 nm [24]

Fig. 2a and 2b depict PEC current of CdSe19h depositions on the four variations of TiO_2 sample, as measured from back-side and front-side illuminations, respectively. The photosensitization of the TiO_2 electrodes in the visible

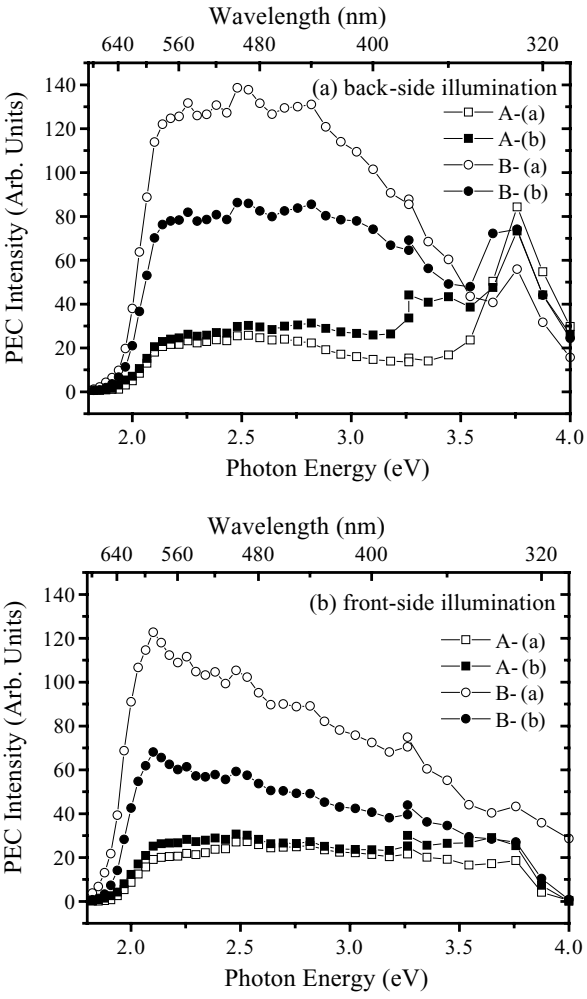

Fig. 2. Photoelectrochemical current spectra of the four formulations of TiO_2 electrode deposited with CdSe quantum dots for 19 h. The measurements were carried out at (a) back-side illumination and (b) front-side illumination, respectively.

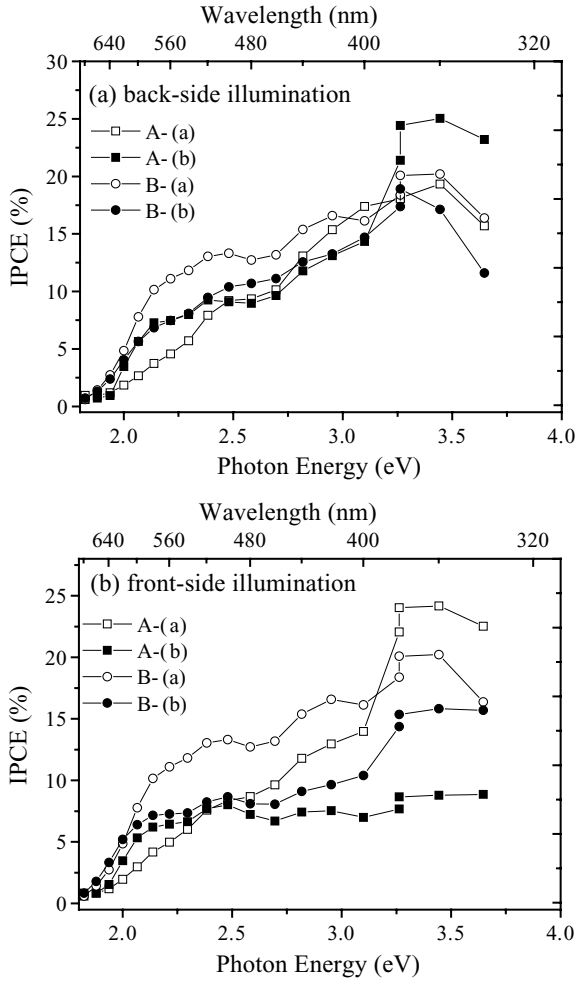

Fig. 3. Incident photon to current conversion efficiency of the four TiO_2 electrodes deposited with CdSe quantum dots with a deposition time of 19 h. The electrolyte was 1 M KCl + 0.1 M Na_2S solution and the measurements were carried out at (a) back-side illumination and (b) front-side illumination, respectively.

region resulting from the CdSe QDs deposition can be clearly observed. The PEC currents in the visible region increased in order of sample A-(a) (15 nm with PEG20000), A-(b) (15 nm with PEG500000), B-(b) (27 nm with PEG500000) and B-(a) (27 nm with PEG20000) when illuminated from either side. The difference in spectra measured at the back-side and front-side illuminations for each sample can be also observed in Fig. 2. The reduction in the PEC current for front-side illumination compared to back-side illumination, especially in the higher photon energy region where the optical absorption coefficient is increased, can be explained by recombination losses during the transport of electrons from surface of the electrode to the back contact. Fig. 3 shows the IPCE measured from back-side (a) and front-side (b) illumination. As in the case of the PEC current, IPCE of the electrode B-(a) (27 nm with PEG20000) is largest in the four sample variations. In order to explain these results, we need to study the microstructure and electron transport of each of the four electrode samples.

3.2. Microstructure and electron transport of the TiO_2 electrodes

Fig. 4 shows the micrographs of scanning electron microscopy (SEM) of each of the four electrode samples. Highly porous nanostructures in the TiO_2 films were apparent from the SEM observations. The average size of the TiO_2 nanocrystals in the electrodes was found to be 50–60 nm for A-(a) (15 nm with PEG20000), 20–30 nm for A-(b) (15 nm with PEG500000) and from a few tens nm to 100 nm for B-(a) (27 nm with PEG20000) and B-(b) (27 nm with PEG500000). The porosity and pore sizes of B-(a) and B-(b) were larger than those of A-(a) and A-(b). These results indicate that the microstructures of the TiO_2 electrodes depend on the TiO_2 nanoparticle size and the MW of PEG in the TiO_2/water paste. Since samples B-(a) and B-(b) have larger porosity and pore size in the TiO_2 microstructures than those of A-(a) and A-(b), we can suppose that more CdSe QDs may be deposited on the surfaces of the TiO_2 nanoparticles. Thus, the larger PEC current in the visible region which occurred in B-(a) and B-(b) could be predicted. As seen from Fig. 2, PEC current of B-(a) is larger than that of B-(b). Since their microstructures appear to be similar, we need also to consider the difference of electron transport processes in the samples.

In a previous work [12], we reported qualitative results of PCT for the four TiO_2 electrode preparations. We found that the photoelectrochemical current peak intensities of samples A-(a) and A-(b) were a few tens of times greater that those of samples B-(a) and B-(b) and that the electron diffusion

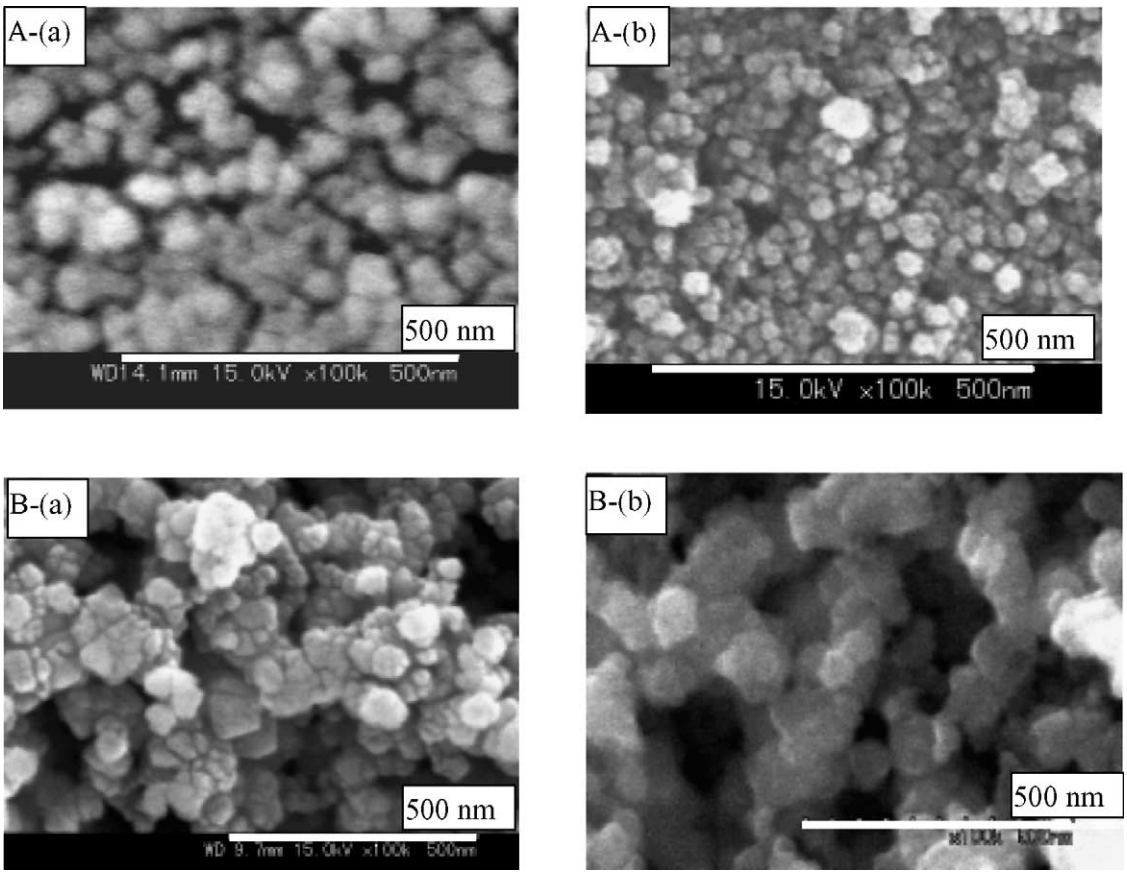

Fig. 4. Micrographs of scanning electron microscopy of TiO_2 electrode samples A-(a) (15 nm with PEG20000), A-(b) (15 nm with PEG500000), B-(a) (27 nm with PEG20000) and B-(b) (27 nm with PEG500000).

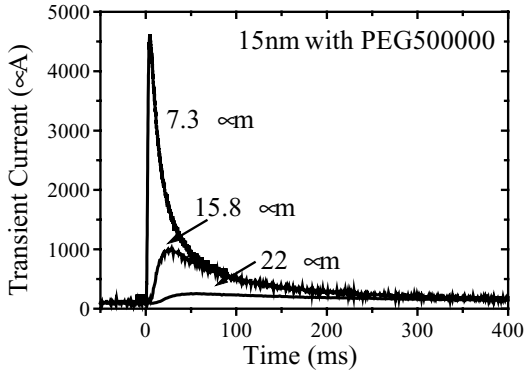

Fig. 5. Photoelectrochemical current transients of A-(b) (15 nm with PEG500000) for different electrode thicknesses.

coefficient in the former is larger than the latter by about almost one order. In this paper we present more detailed results.

Figs. 5 and 6 depict examples of PCT for A-(b) (15 nm with PEG500000) and B-(b) (27 nm with PEG500000) with different film thicknesses, respectively. A single current peak is clearly visible in all transients. The position of the peak (t_{peak}) is shifted to a longer time and the peak current amplitude decreases with increasing film thickness, i.e., with the increased distance of electron travel. Using a diffusion model [19,20], electron diffusion coefficients, D, in the TiO_2 nanostructured electrodes can be determined from the following relation between t_{peak} and the film thickness h:

$$t_{peak} = \frac{h^2}{6D} \quad (1)$$

Figs. 7 and 8 show the dependence of the square of the thickness h^2 on the peak position of the photocurrent transients t_{peak} for samples A-(b) (15 nm with PEG500000) and B-(b) (27 nm with PEG500000), respectively. The electron diffusion coefficients are calculated from the slopes of the lines as 1.5×10^{-5} cm^2/s for A-(b) (15 nm with PEG500000) and 0.66×10^{-5} cm^2/s for B-(b) (27 nm with PEG500000). Using the same method, the electron diffusion coefficients

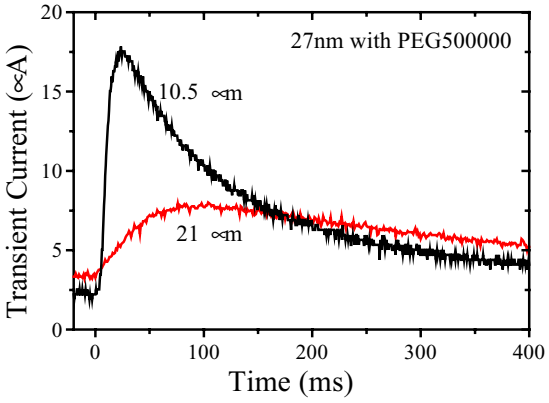

Fig. 6. Photoelectrochemical transients of B-(b) (27 nm with PEG500000) for different electrode thicknesses.

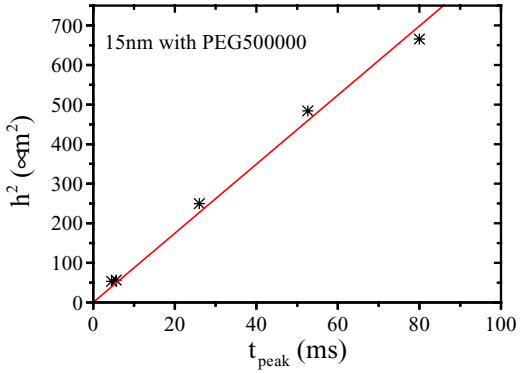

Fig. 7. Dependence of the square of the thickness, h^2, on the peak position of the photocurrent transients t_{peak} for sample A-(b) (15 nm with PEG500000).

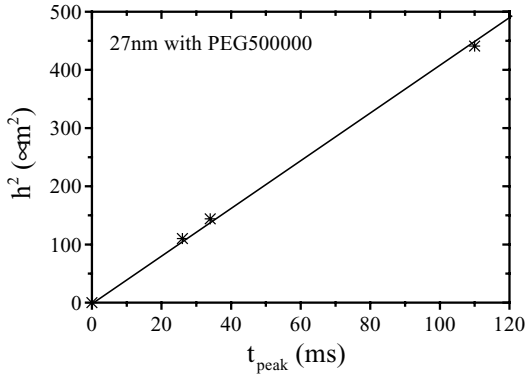

Fig. 8. Dependence of the square of the thickness h^2 on the peak position of the photoelectrochemical current transients t_{peak} for sample B-(b) (27 nm with PEG500000).

for samples A-(a) (15 nm with PEG20000) and B-(a) (27 nm with PEG20000) are 1.5×10^{-5} and 0.96×10^{-5} cm^2/s, respectively. These results are shown in Table 1, indicating that the electron transport properties in the electrodes are largely dependent on the TiO_2 nanoparticle sizes in the TiO_2/water paste and also on the MW of the PEG, in the case of larger TiO_2 nanoparticles.

With samples A-(a) and A-(b), the PEC currents in the visible region were smaller, although they have larger electron diffusion coefficients. This is because the porosity and pore size in their microstructure are so small that few CdSe QDs can be adsorbed. Samples B-(a) and B-(b) each have a similar porosity and pore size. Thus, the fact that the largest PEC current in visible region occurred in B-(a) (27 nm with

Table 1
Electron diffusion coefficient of four formulations of TiO_2 substrate

TiO_2 substrate	D ($\times 10^{-5}$ cm^2/s)
A-(a) (15 nm, PEG20000)	1.5
A-(b) (15 nm, PEG500000)	1.5
B-(a) (27 nm, PEG20000)	0.96
B-(b) (27 nm, PEG500000)	0.66

PEG20000) may be due to a larger electron diffusion coefficient than that in B-(b) (27 nm with PEG500000).

4. Conclusion

Four formulations of nanostructured TiO_2 electrodes, deposited with CdSe QDs by chemical deposition, have been characterized using PA, PEC current spectra and IPCE measurements. The TiO_2 electrodes were prepared with different sized TiO_2 nanocrystalline particles (15 and 27 nm in diameter) and PEG with different MW (20,000 and 500,000). Photosensitization by the CdSe nanoparticles was observed from both the PA and PEC results. It is found that the PEC current in the visible region depends strongly on the microstructure and the electron diffusion coefficient in the TiO_2 electrodes. The TiO_2 electrode B-(a) (27 nm with PEG20000) exhibits largest intensities of the PEC current and IPCE in the visible region. Electron transport processes were studied for the TiO_2 electrodes without CdSe adsorption using transient photocurrent measurements. The electron diffusion coefficient is observed to range between 0.66×10^{-5} and 1.5×10^{-5} cm^2/s for the four formulations of electrode. Based on the above results, we can state that PEC currents in the visible region in the CdSe-sensitized TiO_2 nanostructured electrodes will be largely dependent on both the microstructure and electron diffusion coefficient in the electrodes.

Acknowledgements

Part of this work was supported by a Grant-in Aid for Scientific Research (nos.14750645 and 15510098) and also that on Priority Area (417, no. 15033224) from the Ministry of Education, Culture, Sports, Science and Technology (MEXT) of the Japanese Government. Part of this work was carried out under the 21st Century COE program on "Coherent Optical Science."

References

[1] B. O'Reagan, M. Grätzel, Nature 353 (1991) 737.
[2] M.K. Nazzerruddin, A. Kay, I. Podicio, R. Humphy-baker, E. Muller, P. Liska, N. Vlachopoulos, M. Grätzel, J. Am. Chem. Soc. 115 (1993) 6382.
[3] S. Yanagida, T. Kitamura, M. Kohmoto, Electrochemistry 70 (2002) 399.
[4] C.J. Barbe, F. Arendse, P. Comte, M. Jirousek, F. Lenzmann, V. Shklover, M. Grätzel, J. Am. Ceram. Soc. 80 (1997) 3157.
[5] S. Uchida, M. Tomiha, N. Masaki, Electrochemistry 70 (2002) 466.
[6] R. Vogel, K. Pohl, H. Weller, Chem. Phys. Lett. 174 (1990) 241.
[7] R. Vogel, P. Hoyer, H. Weller, J. Phys. Chem. 98 (1994) 3183.
[8] T. Toyoda, K. Saikusa, Q. Shen, Jpn. J. Appl. Phys. 38 (1999) 3185.
[9] T. Toyoda, J. Sato, M. Hayashi, Q. Shen, Rev. Sci. Instrum. 74 (2003) 297.
[10] L.M. Peter, D.J. Riley, E.J. Tull, K.G.U. Wijayanta, Chem. Commun. 2002 (2002) 1030.
[11] D.F. Underwood, T. Kippeny, S.J. Rosenthal, Eur. Phys. J. D 16 (2001) 241.
[12] Q. Shen, T. Toyoda, Thin Solid Films 438–439 (2003) 167.
[13] A. Rosencwaig, A. Gersho, J. Appl. Phys. 47 (1976) 64.
[14] D.P. Almond, P.M. Patel, Photothermal Science and Techniques, Chapman & Hall, London, 1996, pp. 119–148.
[15] T. Toyoda, T. Takahashi, Q. Shen, J. Appl. Phys. 88 (2000) 6444.
[16] T. Toyoda, J. Sato, Q. Shen, Jpn. J. Appl. Phys. 40 (2001) 3583.
[17] T. Toyoda, M. Hayashi, J. Sato, Q. Shen, Jpn. J. Appl. Phys. 41 (2002) 3367.
[18] T. Toyoda, M. Hayashi, Q. Shen, Jpn. J. Appl. Phys. 42 (2003) 3036.
[19] A. Solbrand, H. Lindstrom, H. Rensmo, A. Hagfeldt, S. Lindquist, A. Sodergren, J. Phys. Chem. B 101 (1997) 2514.
[20] S. Nakade, S. Kambe, T. Kitamura, Y. Wada, S. Yanagida, J. Phys. Chem. B 105 (2001) 9150.
[21] S. Gorer, G. Hodes, J. Phys. Chem. 98 (1994) 5338.
[22] M.G. Bawendi, A.R. Kortan, M.L. Steigerwald, L.E. Brus, J. Chem. Phys. 91 (1989) 7282.
[23] Q. Shen, T. Toyoda, Jpn. J. Appl. Phys., 43 (2004), in press.
[24] X.C. Ai, R. Jin, C.B. Ge, J.J. Wang, Y.H. Zou, X.W. Zhou, X.R. Xiao, J. Chem. Phys. 106 (1997) 3387.